THE ASTROPHYSICAL JOURNAL, 391:736–749, 1992 June 1

PULSATIONAL STUDY OF BL HERCULIS MODELS. I. RADIAL VELOCITIES

J. ROBERT BUCHLER AND PAWEŁ MOSKALIK[1]
Physics Department, University of Florida, Gainesville, FL 32611
Received 1991 September 9; accepted 1991 November 20

ABSTRACT

The linear and nonlinear pulsational behavior of nine sequences of BL Herculis models is studied, and their radial velocity curves are discussed in detail. The pulsations of these stars, in analogy to the classical Cepheids, are strongly affected by internal resonances, most importantly the 2:1 resonance with the second overtone. This latter coupling causes a characteristic systematic progression of the Fourier phases and amplitude ratios as the period ratio P_2/P_0 is varied. In contrast to Cepheids, the strength of the resonance depends very sensitively on the stellar mass and luminosity, and the morphology of the Fourier progression changes significantly when M or L are varied.

In most of the model sequences we find narrow windows in which the pulsations exhibit periodic alternations of deep and shallow minima in the radial velocity and light curves. This behavior occurs for periods somewhere in the range from $2^d.0$ to $2^d.6$, depending on the sequence. It is caused by the 3:2 resonance between the fundamental mode and the first overtone. In the two most nonadiabatic sequences the same resonance causes windows of chaotic oscillations.

Subject headings: Cepheids — stars: oscillations — stars: variables: other

1. INTRODUCTION

The BL Herculis–type variables form a small but interesting group of radially pulsating Population II stars with periods in the range 1^d–3^d. They are observed both in the globular clusters and in the Galactic field and are believed to be on one of the crossings of the instability strip in their post–horizontal branch evolution (e.g., Becker 1985). The properties of these objects have recently been reviewed by Harris (1985), by Wallerstein (1990) and by Wallerstein & Cox (1984), who also give ample references to the literature. In a nutshell, the BL Her variables are the older, smaller, and fainter siblings of the classical (Population I) Cepheids and, as such, they share some of their pulsational properties. It is therefore of interest to survey the oscillatory behavior of the BL Her models in some detail and to make a thorough comparison with their Population I relatives.

One of the most striking features observed in the classical Cepheids is the so-called Hertzsprung progression (Hertzsprung 1926). It has been loosely defined as the occurrence and systematic change with period of a secondary bump or shoulder on the light curves (e.g., Fig. 5 in Ledoux & Walraven 1958). The change can be described in an accurately quantifiable way with a Fourier decomposition technique (Simon & Lee 1981). When this technique is applied to large observational samples of Cepheid light curves (e.g., Simon & Moffett, 1985) or radial velocity curves (e.g., Kóvacs, Kisvarsányi, & Buchler 1990) it unveils a strong and very characteristic correlation of the Fourier parameters with the pulsation period, especially well defined for the low-order Fourier phases.

An extended systematical survey of the nonlinear classical Cepheid models has recently been performed with special attention to the behavior of the Fourier parameters. This numerical hydrodynamical study (Buchler, Moskalik & Kovács 1990, hereafter BMK) has shown that within a wide range of luminosities and masses, the Fourier phases for the radial velocities and for the light curves display an *almost universal* behavior along the sequences of models. The fact that this quasi-universal behavior is correlated with the period ratio, $P_{20} \stackrel{\text{def}}{=} P_2/P_0$, but not with the period P_0, provides strong evidence that *the progression of the phases has its origin in the* 2:1 *resonance* between the fundamental mode and the second overtone. The correlation of the bump location with this resonance was first suggested by Simon & Schmidt (1976). The recently developed *amplitude equation formalism* (Buchler & Goupil 1984; Buchler 1985) provides an analytical framework within which the progression of the Fourier coefficients can indeed be shown to be a manifestation of the 2:1 resonance (Klapp, Goupil, & Buchler 1985; Buchler & Kovács 1986). Furthermore, with the help of this formalism, the variations of the Fourier parameters with the distance to the resonance center are also captured very well *quantitatively* (Kovács & Buchler 1989; hereafter KB89).

The question arose naturally whether a bump progression, similar to the one witnessed in classical Cepheids, is also present in the Cepheids of Population II (Stobie 1973). It seems, however, that the occurrence of such a progression in the BL Her variables is less clear. The observed light curves still show an eyeball correlation of the position of a "bump" with period (descending vs. ascending branch) with a changeover in the vicinity of $1^d.5$–$1^d.7$ (Petersen 1981; Carson, Stothers, & Vemury 1981; Carson & Stothers 1982). However, the variation of the Fourier parameters is not very characteristic, and it is therefore not astonishing that various analyses have arrived at differing conclusions (Petersen & Diethelm 1986; Simon 1986; Carson & Lawrence 1987). The situation is even less clear for the radial velocity curves which are too poorly sampled to even discuss the presence or absence of a progression.

There was a brief interval of interest in the nonlinear pulsations of BL Her models in the past (King, Cox, & Hodson 1981; Carson et al. 1981; Carson & Stothers 1982; Hodson,

[1] Permanent address: Copernicus Astronomical Center, ul. Bartycka 18, 00-716 Warsaw, Poland.

Cox, & King 1982; Carson & Lawrence 1987). Unfortunately, in all these studies the combinations of stellar parameters, i.e., masses, luminosities, and effective temperatures, were chosen in a way which made any systematical behavior difficult to detect. We have therefore perceived the need to survey the nonlinear behavior of BL Her models from a different perspective. Our approach (similar to BMK's) again concentrates on *sequences* of models, i.e., families in which *only one* stellar parameter is varied (in our case $T_{\rm eff}$). The procedure of combining such systematical numerical studies with an analytical formalism has already met with some success in explaining features of the nonlinear pulsations in other stars (the Hertzsprung progression in classical Cepheids, already mentioned; double mode behavior in RR Lyrae models; RV Tauri–like alternating pulsations in Cepheid models; the transition from regular to irregular [chaotic] oscillations in W Vir models; for a review of these topics, cf. Buchler 1990).

This is the first of two papers in which we discuss the results of an extensive and systematic survey of BL Her models. In this manner the effects of the resonances on the oscillations of these stars will be clearly exhibited. Paper I presents the nonlinear pulsational behavior of nine sequences of models and interprets this behavior in terms of their linear properties (linear period ratios and growth rates). Because we are primarily interested here in the dynamics of the oscillations, we concentrate on the radial velocity variations. In Paper II, we shall discuss the light curves of the models and shall compare them with the available observational data. We remark that the main purpose of our survey is a study of the *systematics* of the nonlinear pulsating models, rather than an attempt to model any specific BL Her–type star.

2. MODEL SEQUENCES

We have constructed the BL Her model sequences as one-parameter families in which the luminosity, mass and composition are held constant, and in which the $T_{\rm eff}$ is the control parameter which is varied. We have analyzed in some detail nine such sequences whose parameters are summarized in Table 1. The luminosities of sequences A–G span the observed range from 100 $L_\odot$ to 175 $L_\odot$ (e.g., Demers & Harris 1974) and the masses the "canonical" range of 0.55 $M_\odot$ to 0.65 $M_\odot$. We have added sequence H with $L = 200\ L_\odot$ for completeness and to allow for observational uncertainty. The adopted composition is typical of metal-poor Population II stars for all sequences except for F. For comparison, and because the BL Her stars display a wide range of metallicities, the latter sequence has been constructed with the same parameters as sequence B, but with a Population I metal content. Finally, sequence I has a very low mass of 0.4 $M_\odot$, and its composition is that of the W Vir models studied by Kovács & Buchler (1988b). We note that {A, B, C, G, H} form a fixed-mass group of sequences; this allows one to see the change in pulsational behavior with increasing luminosity (or nonadiabaticity). Similarly, the fixed-luminosity group of sequences {B, D, E} permits a study of the effect of varying the mass.

All our models are purely radiative. This is a good approximation at the higher $T_{\rm eff}$, but at the lower $T_{\rm eff}$ time-dependent convection is expected to play an important role, and our cooler models are perhaps not realistic. In fact, convection is believed to provide the damping which is responsible for the existence of a red edge, which the radiative models do not reproduce. Some of the sequences have nevertheless been computed to low $T_{\rm eff}$ (unreasonably low from an observational viewpoint), mostly in order to study the dynamical effects of the $\omega_1 = 2\omega_0$ and $\omega_2 = 3\omega_0$ resonances which have aroused some interest in the past (Carson et al. 1981; Cox 1984; Cox & Kidman 1985). [Here the $\omega_k = 2\pi/P_k$ represent the imaginary parts of the complex eigenvalues, $\sigma_k = i\omega_k + \kappa_k$, of the (linear) normal modes of vibration, for an assumed $\exp(\sigma t)$ time-dependence.]

All sequences have been studied with an affordable, but relatively coarse resolution of 60 zones. The model envelopes all extend inward to 2×10^6 K. Our hydrodynamical code (Kovács & Buchler 1988a) is essentially that of Stellingwerf (1974, 1975) which treats shocks with an artificial viscosity ($C_Q = 4$, $\alpha = 0.01$). This scheme is most accurate for a constant time step and we have taken the latter to be a 1/600 of the period for sequences A and B and 1/200 of the period for sequences C–I. For the periodic pulsations (limit cycles) of the models, the dynamical behavior has generally been computed to a periodicity of better than 10^{-4}. This is achieved through an iterative relaxation to the exact limit cycle (Stellingwerf 1974) which yields at the same time the Floquet stability coefficients of the computed solution. The method is sufficiently powerful to converge even when the resultant limit cycle is mildly unstable. In all our calculations Stellingwerf's (1975) analytical opacity formula, based on the Los Alamos tables, is used. As in the past (Buchler 1990), we stress that it is imperative that the linear and nonlinear studies use the *same numerical mesh* and the *same input physics* if a meaningful correlation is to be made between the linear resonance properties and the nonlinear dynamical behavior. The price to pay, however, is that because of the coarse mesh and shallow envelopes, the *linear* properties, i.e., periods and growth rates, are then relatively poorly determined for given stellar parameters L, M, and $T_{\rm eff}$. We have therefore imposed an anchor by requiring that in

TABLE 1

PARAMETERS OF THE MODEL SEQUENCES

Sequence	Symbol	$M/M_\odot$	$L/L_\odot$	X	Z	ξ
A	○	0.60	100	0.700	0.001	226
B	□	0.60	125	0.700	0.001	283
C	△	0.60	150	0.700	0.001	340
D	✳	0.55	125	0.700	0.001	325
E	✧	0.65	125	0.700	0.001	249
F	×	0.60	125	0.700	0.020	283
G		0.60	175	0.700	0.001	396
H		0.60	200	0.700	0.001	452
I		0.40	100	0.745	0.005	433

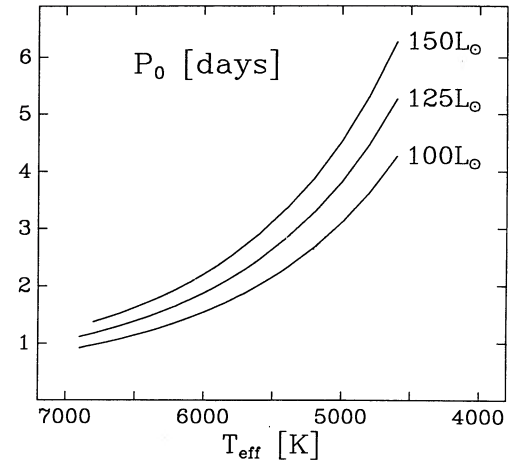

FIG. 1.—Linear period of the fundamental mode vs. $T_{\rm eff}$ for sequences A, B, and C.

all static models a specified zone (45) always be exactly at a specified temperature (here at 15,000 K, except for sequence I for which it is 11,000 K). The anchor has been calibrated to give a rough agreement with growth rates computed with a finer mesh. This procedure has been shown to give consistency between the linear growth rates and the growth rates extracted from a hydrodynamical integration of the model when initiated with a small amplitude (Kovács 1990). In any case, our fundamental mode blue edges ($\kappa_0 = 0$) are in a reasonable agreement with the observationally derived ones (Demers & Harris 1974); they also agree within 100 K with the theoretical blue edges of King et al. (1981).

Figure 1 displays the fundamental mode linear periods, $P_0 = 2\pi/\omega_0$, as a function of $T_{\rm eff}$ for model sequences A–C, and Figure 2 presents the fundamental mode growth rates, $\eta_0 = 2\kappa_0 P_0$, for the same sequences (in our convention the mode is stable [unstable] when κ is negative [positive]). We note that, just as for the classical Cepheids (e.g., Fig. 2 of BMK), the growth rates η_0 increase with luminosity, although, in general, for the BL Her models they are already significantly higher than for the Cepheids. In Table 2 we show the temperatures of the fundamental blue edges, $T_{\rm BE}$, for all nine sequences. Since resonances will be seen to be important in the studied models,

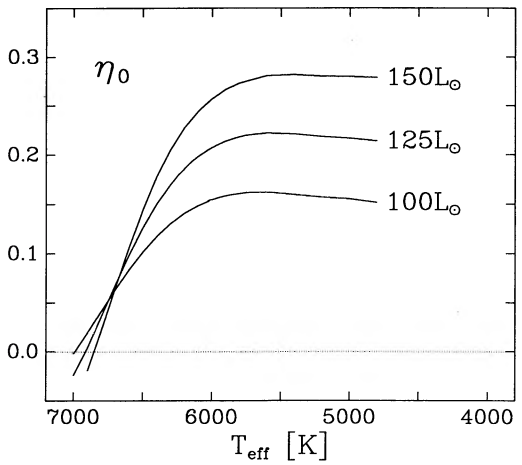

FIG. 2.—Linear growth rate of the fundamental mode vs. $T_{\rm eff}$ for sequences A, B, and C.

TABLE 2

LOW-ORDER RESONANCES IN BL HER MODELS

Sequence	$T_{\rm BE}$ (K)	$\omega_4 = 3\omega_0$ (K)	$\omega_2 = 2\omega_0$ (K)	$2\omega_1 = 3\omega_0$ (K)	$\omega_3 = 3\omega_0$ (K)
A.....	6990	6160	5960	5560	5190
		(1.40)[a]	(1.58)	(2.07)	(2.71)
B.....	6910	6240	6160	5760	5400
		(1.61)	(1.69)	(2.20)	(2.83)
C.....	6850	6300	6300	5920	5560
		(1.82)	(1.82)	(2.32)	(2.98)
D.....	6890	6310	6300	5920	5550
		(1.64)	(1.66)	(2.11)	(2.73)
E.....	6940	6180	6020	5620	5250
		(1.58)	(1.75)	(2.28)	(2.97)
F.....	6830	6240	6120	5640	5120
		(1.63)	(1.74)	(2.35)	(3.37)
G.....	6800	6370	6400	6060	5680
		(2.00)	(1.96)	(2.43)	(3.15)
H.....	6760	6450	6460	6170	5750
		(2.13)	(2.13)	(2.54)	(3.36)
I.....	6780	6600	6520	6270	5780
		(1.45)	(1.52)	(1.77)	(2.45)

[a] Periods, in days, are given in parentheses.

we also present the locations (i.e. $T_{\rm eff}$ and P_0) of the four lowest order linear resonances.

3. HYDRODYNAMIC RESULTS

3.1. *Radial Velocity Curves*

Figure 3 exhibits the radial velocity curves (in the theorists' convention, $V_r = +dR/dt$, no limb darkening corrections) as a function of phase for selected models of the sequences A, B, and C. The various curves are shifted vertically for better display. The labels refer to the $T_{\rm eff}$ [K] of the static models and to the nonlinear pulsation periods [day], respectively. A systematic progression of the shapes of the velocity curves with period is clearly visible. In all three sequences a prominent bump feature appears first on the descending part of the curve, then with increasing period it moves to earlier phases of the pulsation cycle, and finally switches to the ascending part of the curve after the center of the $\omega_2 = 2\omega_0$ resonance is crossed. Such a change in the morphology of the limit cycles suggests that the resonance is instrumental in their shaping. We should note, however, that in each of the sequences the resonance occurs at a *different period* (cf. Table 2) and, as a result, *at any given period, differing shapes of the radial velocity curves are possible* (compare e.g., models with $P_0 = 1^{\rm d}.74$).

The progression observed in sequence A is remarkably similar to that found both in the theoretical models of classical Cepheids (BMK, their Fig. 4), and, we may add, in the Cepheid observations (Kovács, Kisvarsányi, & Buchler 1990). In particular, near the center of the 2:1 resonance the bump does not merge with the main maximum, but rather the two maxima trade their roles. In the higher luminosity sequences B and C, though, the behavior is different. In this case the bump seems to disappear on one side of the maximum and simultaneously reappear on another. This results in characteristic double-bump velocity curves in the very center of the resonance. We do not present here the radial velocities for the other six sequences. It suffices to mention that sequences D, E, and F are very similar to sequences C, A, and B, respectively. This resemblance is also seen in the behavior of the Fourier parameters which will be discussed in the next subsection.

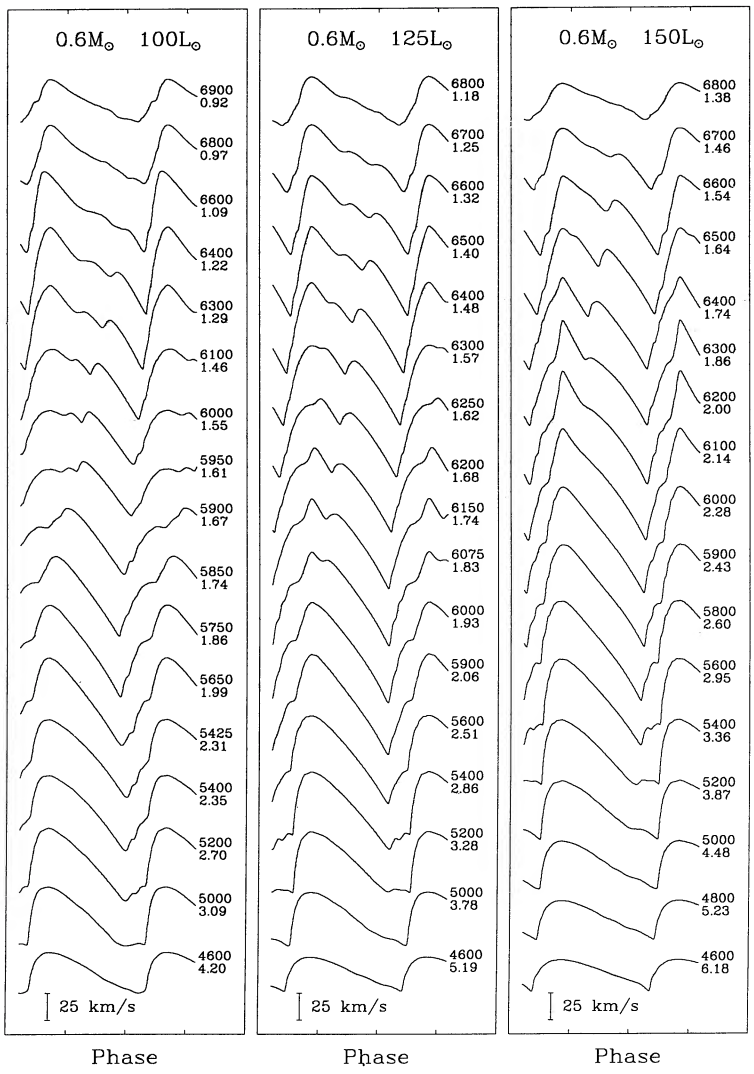

FIG. 3.—Progression of radial velocity curves for sequences A, B, and C; labels on the right denote $T_{\rm eff}$ [K] of the static models and the nonlinear pulsation periods [day].

In Figure 4 we present maximum and minimum velocities for the models of sequences A and C. The open circles correspond to those limit cycles, which are unstable toward a period doubling bifurcation. This instability, giving rise to new limit cycles with alternating maxima and minima (marked by crosses), will be discussed in detail in § 3.5. Figure 4 shows again that the 2:1 resonance strongly influences the pulsations of the models, although a striking difference between the two sequences is seen. In the low-luminosity sequence A the amplitude of the velocity variations, ΔV_r, has a *minimum* at the center of the resonance, which is the same behavior as observed in the models of classical Cepheids. On the other hand, in the resonance center of sequence C a *maximum* of ΔV_r is reached. A qualitative change in the behavior of the BL Her models with the increase of luminosity is, thus, further emphasized.

The highest velocity amplitudes found in sequences A and C are 86 km s^{-1} and 108 km s^{-1}, respectively. When we correct these values for the limb darkening (multiplying by 17/24), we obtain 61 km s^{-1} and 76 km s^{-1}, respectively. Such amplitudes are significantly too large compared to the range of 30–45 km s^{-1} observed in most of bona fide BL Her stars (Fig. 2 of Harris & Wallerstein 1984; cf. however, XX Vir; Wallerstein & Brugel 1979). While the discrepancy has to be examined in detail, we think that it is probably not as serious as might seem at first. We recall that our theoretical velocities are computed for the last, i.e., outermost zone of the numerical models. On the other hand, observed radial velocities are usually determined from the metallic lines which are formed somewhat *deeper* in the stellar atmosphere. Since the range of velocity variations rapidly decreases inward in the models, the difference in depth can account for (at least) part of the discrepancy. This conjecture is further supported by measurements of Abt & Hardie (1960) who have found that the velocity amplitude of BL Herculis, as determined from the hydrogen lines (small optical depth) is by 55%–60% *larger* than the one measured from the iron lines. This result, if applicable to all BL Her–type stars, would bring our theoretical amplitudes into a good agreement with observations.

As far as the bump progression is concerned, unfortunately very little detailed observational information is available. In most cases the velocity curves are poorly sampled and a secure identification of the bump is not even possible. To the best of

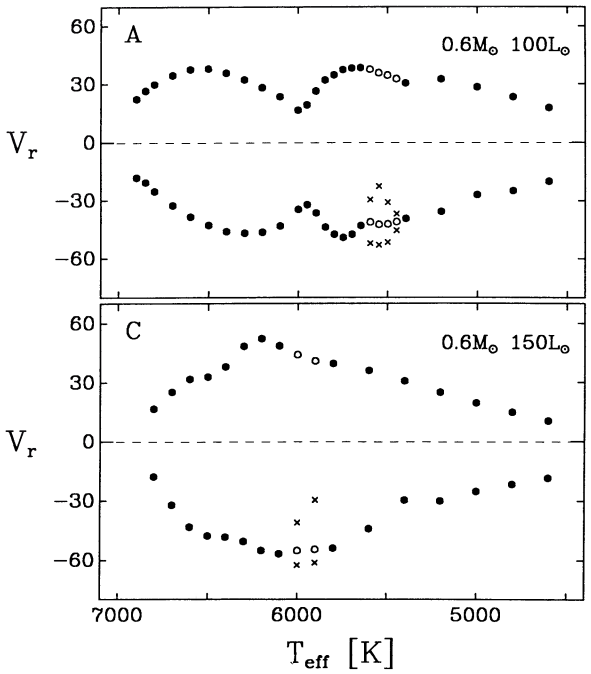

FIG. 4.—Maximum and minimum pulsational velocities vs. $T_{\rm eff}$; *top:* for sequence A and *bottom:* for sequence C. Open circles correspond to models which are unstable toward a period doubling, crosses mark the (alternating) minima of the stable period 2 models.

our knowledge, SW Tau ($P_0 = 1^{\rm d}.58$) is the only BL Her-type variable with a definite velocity bump, occurring ~ 0.4 of a cycle after the primary maximum (Stobie & Balona 1979; Barnes, Moffett, & Slovak 1988). Radial velocity variations observed in this star are similar to those computed for the $1^{\rm d}.46$ model of sequence A or the $1^{\rm d}.57$ model of sequence B (Fig. 3).

3.2. *Fourier Decomposition*

In order to give a more quantitative description of the shape of the pulsation cycle and its change with period we resort to a standard technique of Fourier decomposition. To that effect we fit the temporal behavior of the photospheric *radius* (strictly speaking the outer radius) with a sum of the form

$$A_0^r + \sum A_n^r \sin\,(n\omega t + \phi_n^r)\,. \tag{1}$$

The composite Figure 5 displays the first two relative Fourier phases ϕ_{21} and ϕ_{31} as well as the amplitude ratios R_{21} and R_{31}, for sequences A–C ($R_{n1} \overset{\rm def}{=} A_n/A_1$ and $\phi_{n1} \overset{\rm def}{=} \phi_n - n\phi_1$). Similarly, the composite Figures 6 and 7 show the same Fourier parameters for sequences D–F and G–I, respectively. The corresponding Fourier parameters for the radial velocities (in the observers' convention, i.e., $V_r = -dR/dt$) can be obtained as

$$\phi_{n1}^v = \phi_{n1}^r + (n-1)\pi/2\,, \tag{2}$$

$$R_{n1}^v = nR_{n1}^r\,, \tag{3}$$

In all three figures the solid dots correspond to the stable pulsations, and the open circles represent the limit cycles which are unstable toward a period doubling, as in Figure 4. It will be seen that internal resonances among the normal modes of oscillation play an important role in shaping the pulsations of the models. Therefore, in the bottom parts of Figures 5–7 we display the ratios of the linear growth rates for the low-order resonant overtones and indicate the positions of the integer resonances with dots.

In all the sequences the Fourier amplitudes and phases show systematical variations with $T_{\rm eff}$. These variations are smooth, with exception of sequences H and I in which a discontinuity occurs around $T_{\rm eff} \simeq 6400$ K. Because we have attached a great deal of importance to stability in the numerical computations (Buchler 1990) we believe that all the features seen in Figures 5–7 are real. In the following we will address the most important of our results:

1. The Fourier coefficients gradually deform as the luminosity is increased from 100 $L_\odot$ to 200 $L_\odot$ in sequences {A, B, C, G, H}, all of which have the same mass and standard Population II composition. A gradual change in the Fourier progression is also seen when a stellar mass is varied at constant L (sequences {D, B, E}). An increase in M has qualitatively the same effect as a decrease in L.

The change in the metal content has a rather small influence on the oscillatory behavior of the models. Comparison of sequence B and F shows that the increase of Z lowers the maxima of the R_{21} and R_{31} curves, and slightly increases the peak of ϕ_{21}. The overall character of the Fourier progression, however, remains almost the same.

2. The set of four sequences {A, B, E, F} displays a similar behavior. The pair of sequences C and D are also akin, but they are substantially different from the first set, especially for the higher order coefficients ϕ_{31} and R_{31}. For all six sequences the Fourier phase ϕ_{31} has the same values at either end of the plot (mod 2π), but it undergoes a variation of 2π for the first four sequences while it is essentially flat for the other two. The results of KB89 show that in the presence of the 2:1 resonance (see below) the variations of the Fourier phases and amplitude ratios can be very sensitive to the model parameters. More technically, they depend rather strongly on the values of the expansion coefficients h_{ij} which change from one sequence to another. It can be demonstrated that, depending on the relative sizes of these coefficients, both types of ϕ_{31} progressions can be accommodated. Finally, we note that the third set of sequences, {G, H, I}, while similar in some respects to the pair {C, D}, displays different behavior of R_{21}, and, in general, has much more structure near the blue edge.

It is interesting to look again at the *empirical dissipation parameter* $\xi = L/M^{1.6}$ that was introduced by BMK. The values of ξ for our BL Her models are given in Table 1. The grouping of the sequences according to ξ leads to precisely the same result as the eyeball inspection of the variations of the Fourier coefficients: the first group {A, B, E, F} with small values of $225 < \xi < 285$, the second one {C, D} with intermediate values of $320 < \xi < 345$ and the third one {G, H, I} with large values of $395 < \xi < 455$.

3. The behavior of the low ξ sequences {A, B, E, F} is dominated by the 2:1 resonance between the fundamental mode and the second overtone. These sequences are characterized by a pronounced "bell-shape" variability of ϕ_{21}, with the maximum occurring nearly exactly at the resonance center. At the same place R_{21} and R_{31} experience a rapid drop, whereas ϕ_{31} monotonically increases. Such progressions of the Fourier parameters are very similar to those seen in the Cepheid models of BMK which are also controlled by the same 2:1 resonance. The height of the ϕ_{21} peak in sequences {A, B, E, F} strongly anticorrelates with the relative damping of the second

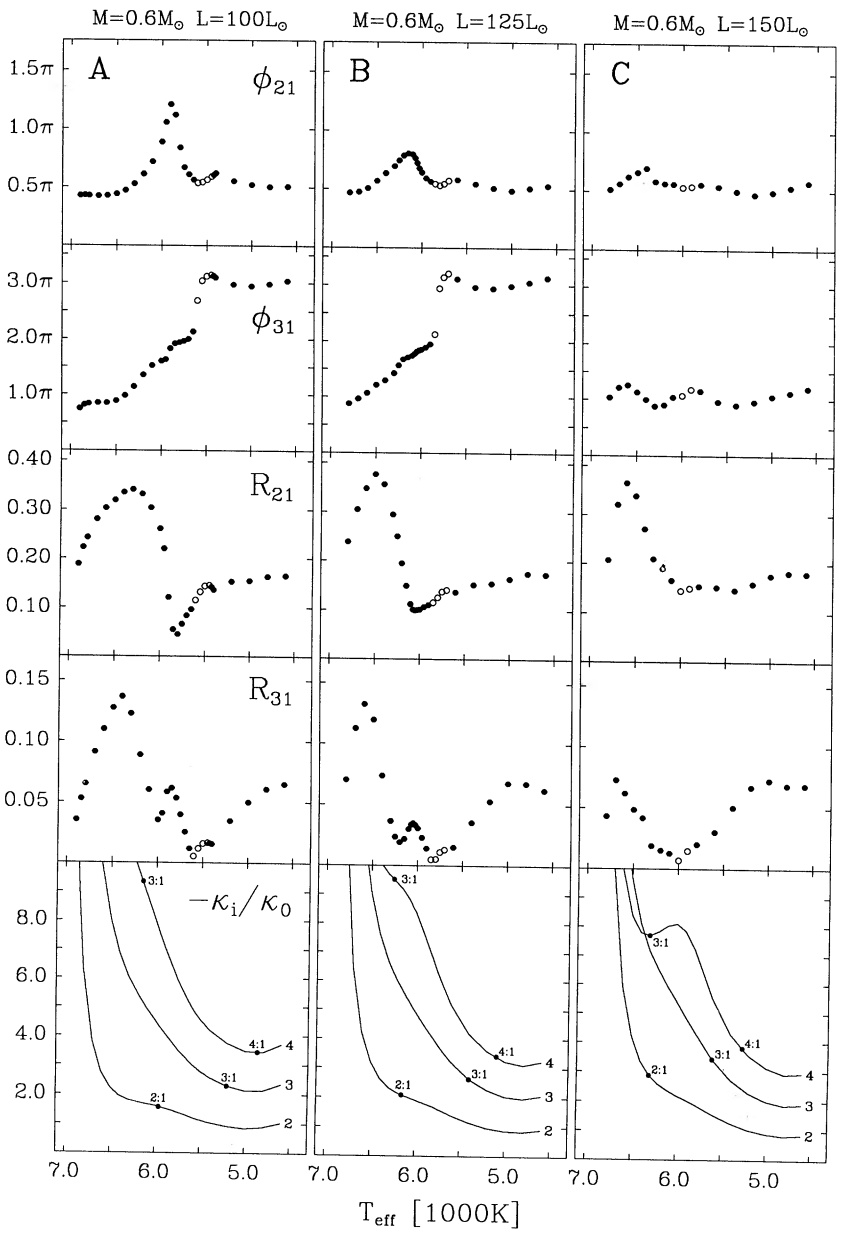

FIG. 5

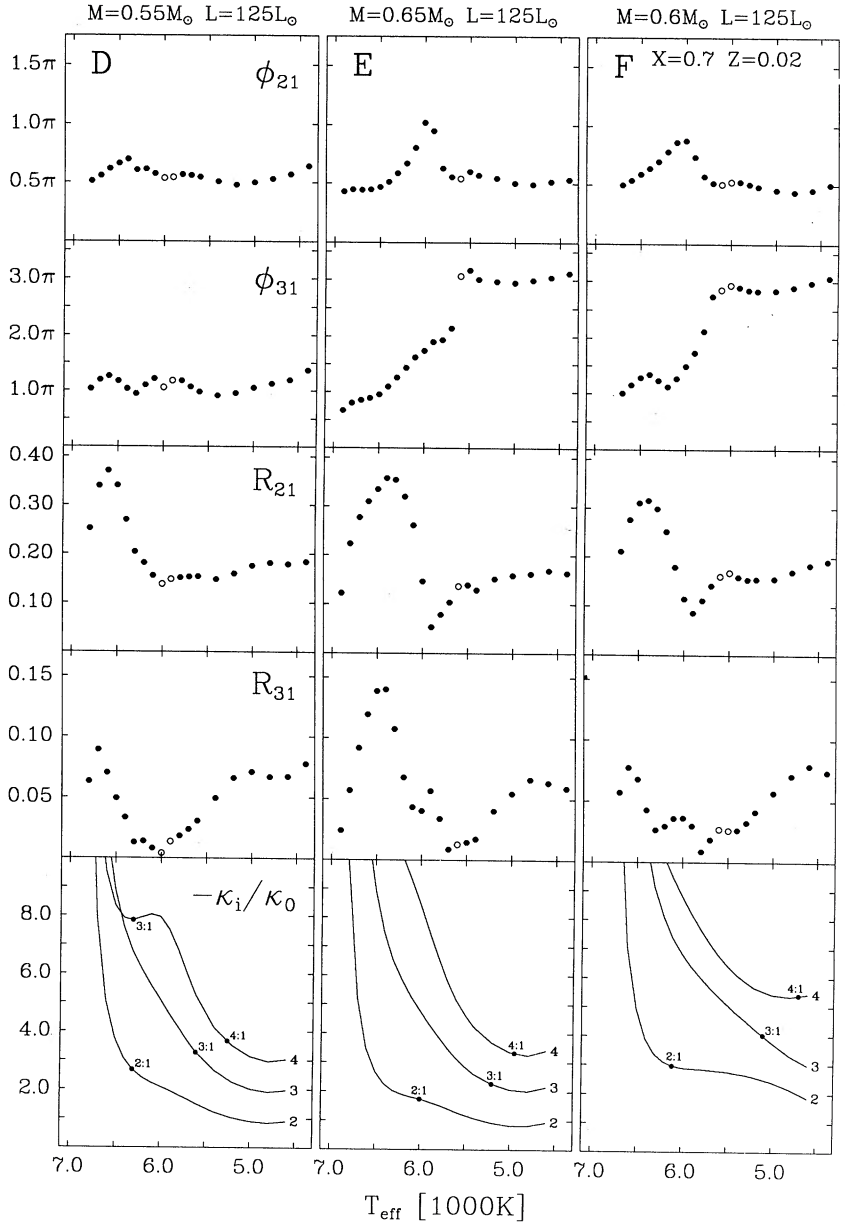

FIG. 6

FIG. 5.—*Top:* Fourier phases and amplitude ratios for the radius variations vs. $T_{\rm eff}$, for sequences A, B, and C. Open circles correspond to unstable limit cycles. *Bottom:* relative growth rates $(-\kappa_i/\kappa_0)$ for the second, third, and fourth overtones. Dots mark positions of integer resonances.

FIG. 6.—Same as Fig. 5, but for sequences D, E, and F

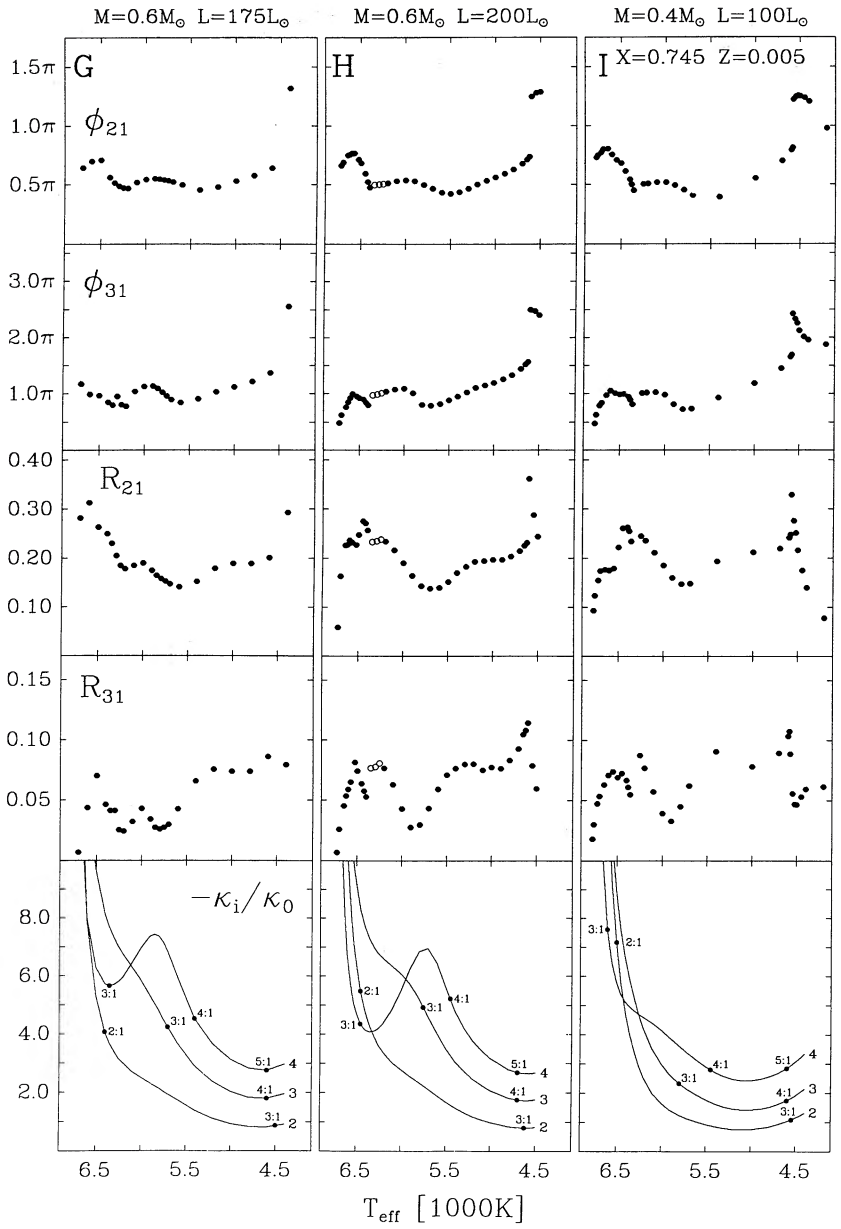

FIG. 7.—Same as Fig. 5, but for sequences G, H, and I

overtone, $|\kappa_2/\kappa_0|$. With an increase of this parameter, the resonant mode becomes more difficult to excite and, consequently, the signature of the resonance is weakened. The same correlation extends also to sequences C and D.

4. In order to put the statement about the similarity between the BL Her and Cepheid models on a *quantitative* ground, we have made a comparison of our sequence A with the sequence D of BMK. The BL Her models are considerably more dissipative; at the resonance center of the sequence A we have $\eta_0 = 2\pi\kappa_0/\omega_0 = -0.152$, whereas for the Cepheid models $\eta_0 = -0.097$. We therefore expect (cf. Buchler & Kovács 1986) that the Fourier parameters display sharper features as a function of the period ratio P_{20} in the Cepheid case. In Figure 8 we plot jointly the BL Her sequence (*filled circles*) and the Cepheid sequence (*open circles*). For the latter, a stretch of the abscissa P_{20} by a factor of 1.5 about $P_{20} = 0.5$ has been applied, as suggested by the above numerology. The similarity of the ϕ_{21}, ϕ_{31}, and R_{21} curves is quite impressive. For the amplitude ratios R_{31}, a significant difference between the two sequences is observed at $P_{20} > 0.49$. We shall return to this point in § 3.4. We recall in passing that the great similarity between the sequences displayed in Figure 8 has already been noted in § 3.1, where the progression of the actual radial velocity curves was discussed.

The values of ξ are very close for the two sequences, but this is probably a pure coincidence. For the classical Cepheid models the behavior of the Fourier coefficients is essentially the same in the broad range of $225 < \xi < 305$, and for larger values of ξ it changes rather slowly (BMK). In contrast, for the BL Her models the sensitivity to ξ is very strong, as Figures 5–7 indicate. Our sequence B and the Cepheid sequence A of BMK, for example, are characterized by nearly the same ξ, but already have quite a different progression of ϕ_{21}. We conclude that while the *trends* with ξ are the same in the BL Her and in

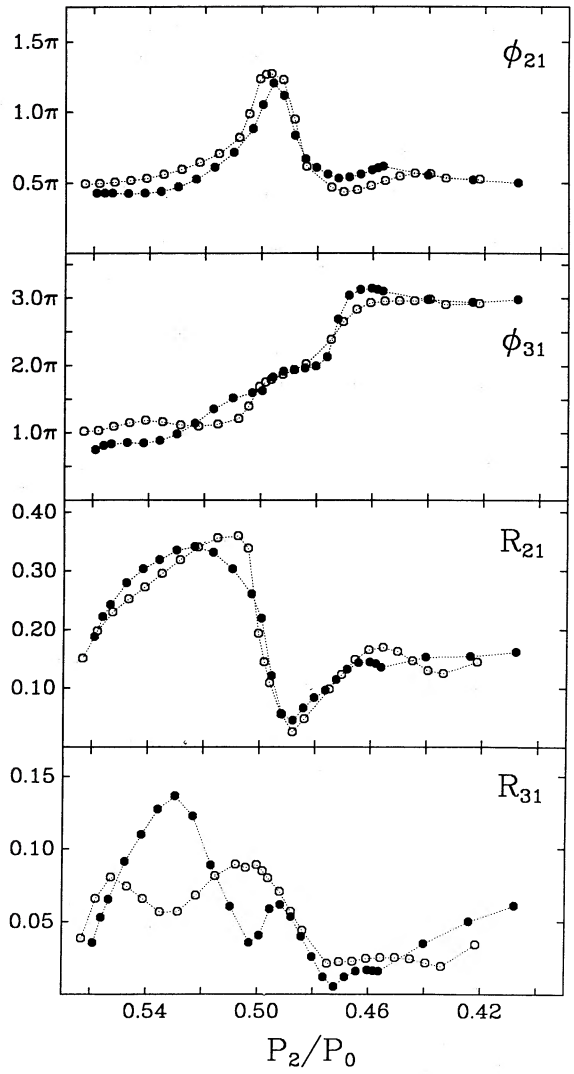

FIG. 8.—Comparison of the BL Her sequence A (*filled circles*) with the classical Cepheid sequence D of BMK (*open circles*). Fourier parameters are plotted vs. period ratio P_{20}; for Cepheid models abscissa is stretched by a factor of 1.5 about the center of the resonance.

the Cepheid models, a comparison of the actual values of ξ between the two types of stars is not meaningful.

5. In the case of the classical Cepheids, in which the $\omega_2 = 2\omega_0$ resonance also plays a dominant role, the model sequences display a quasi-universal behavior when their Fourier parameters are plotted versus P_{20}. In Figure 9 we have similarly replotted as a function P_{20}, the phases and the amplitude ratios (for the *radius* variations) of the models of Figures 5 and 6. While there is still a clear similarity between the sequences, the lack of "*universality*" is most striking in the very resonance region. The reason for the different behavior is that, as pointed out above, the BL Her models are much more sensitive to changes in ξ than the classical Cepheid models.

For comparison with future observational data we also display in Figure 10 the Fourier coefficients of the *radial velocity* curves, now plotted versus the (linear) period P_0.

6. Not only the shape of the Fourier progression, but also the location of the 2:1 resonance are *very* sensitive to *M and* to *L* in the BL Her models. As Table 2 shows, changing the luminosity from 100 $L_\odot$ to 150 $L_\odot$ (at $M = 0.6\ M_\odot$), which is well within the observed range of values, we shift the resonance center from $P_0 = 1^d.58$ to $P_0 = 1^d.82$. Similarly, changing the mass from 0.55 $M_\odot$ to 0.65 $M_\odot$ (at $L = 125\ L_\odot$) we shift the resonance from $P_0 = 1^d.66$ to $P_0 = 1^d.75$.

We also note that in the BL Her case the period ratio P_{20} varies *very quickly* with P_0 or $T_{\rm eff}$. For example, a change of effective temperature by 1000 K (from 6900 K to 5900 K) in our sequence A results in a change in P_0 from $0^d.92$ to $1^d.64$ (i.e. by a factor of 1.78) and in P_{20} from 0.559 to 0.496 (i.e., by 0.063). A comparable change of $T_{\rm eff}$ (from 6000 K to 5000 K) in the Cepheid sequence D of BMK causes a change of P_0 from, $7^d.31$ to $13^d.89$ (a factor of 1.89), but P_{20} varies only by 0.042. Thus, for the BL Her models the lines of P_{20} versus log P_0 are $\sim$60% *steeper* than in the Cepheid case, and the same is also true for other period ratios. As a consequence of this behavior there are more resonances in a comparable range of effective temperatures in the BL Her sequences, which gives rise to a faster change of the morphology of pulsations as the period is varied. In addition, because of the higher packing, the reson-

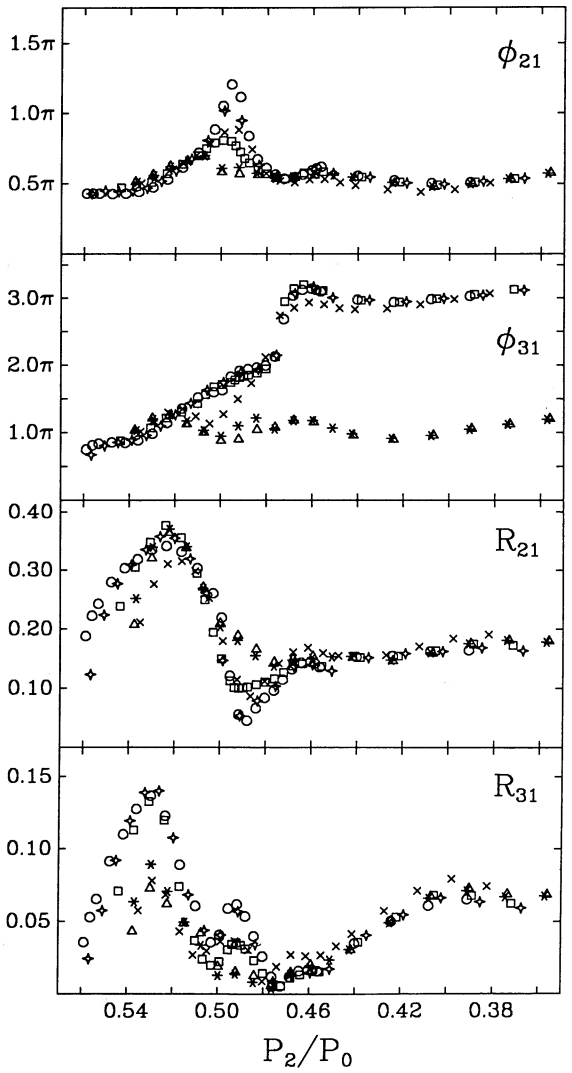

FIG. 9.—Fourier parameters for the radius variations vs. period ratio P_{20} for sequences A–F. Symbols are given in Table 1.

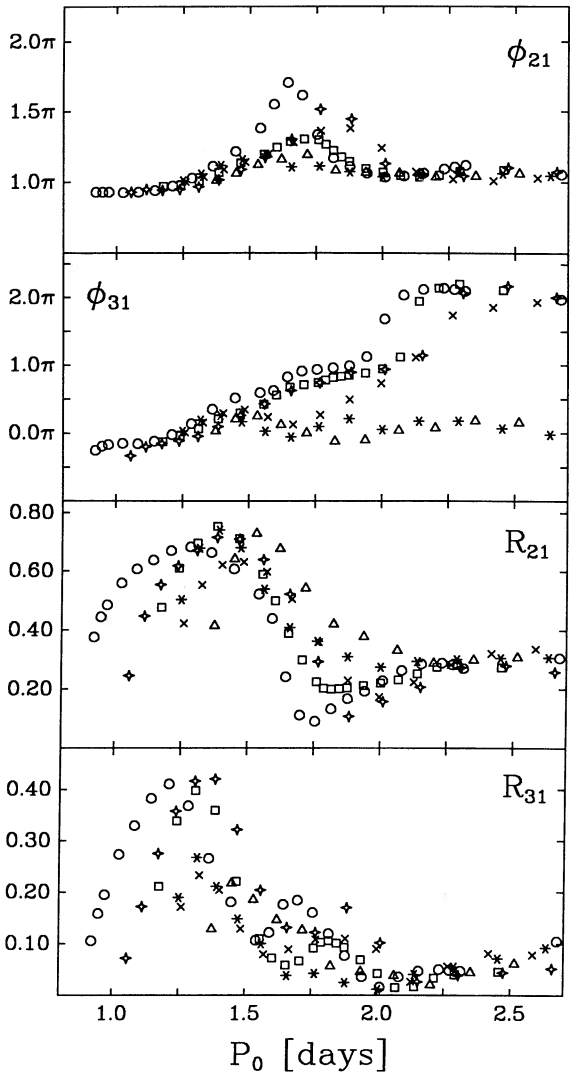

FIG. 10.—Fourier parameters for the *observers' radial velocities* vs. pulsation period P_0 for sequences A–F. Symbols are given in Table 1.

ances have more overlap, so that more complicated pulsational behavior can be expected. This property explains a great amount of structure of the Fourier parameter curves shown in Figures 5–7, compared to the Cepheid case. Particularly important in that context are the 3:1 resonances, two of which occur in our models. The $\omega_3 = 3\omega_0$ resonance is always correlated with a local minimum in ϕ_{31}, and in sequences {G, H, I} also with a minimum in R_{21} and R_{31}. The 3:1 coupling between the fundamental and the fourth overtone, on the other hand, seems to be the cause of a secondary minimum of R_{31} observed in sequences {A, B, D, E, F}. We shall discuss this latter case in detail in § 3.4.

7. Referring back to Figure 7 we note that, in the high ξ sequences {G, H, I} the 2:1 resonance with a second overtone becomes ineffective and, as a result, the Fourier phases ϕ_{21} and ϕ_{31} remain essentially flat throughout most of the $T_{\rm eff}$ range. In the low temperature end of these sequences, though, the integer resonances with consecutive overtones, namely, $\omega_2 = 3\omega_0$, $\omega_3 = 4\omega_0$, and $\omega_4 = 5\omega_0$, have an approximate *accumulation point* (± 100 K), located at $\simeq 4600$ K. Additionally, a 2:1 resonance with the first overtone occurs nearly at the same place. Because this latter mode does not have any resonances in the astrophysically interesting range of effective temperatures, we have not displayed its relative growth rate in the Figures 5–7. Nevertheless, this mode is always either unstable or has the lowest damping of all the overtones.

The coincidence of all integer resonances at essentially one $T_{\rm eff}$ can be interpreted in terms of a polytropic model. It was shown empirically (Simon & Sastri 1972) that in such a model the period ratios satisfy a relation of the form $P_k/P_l = (b + l)/(b + k)$, where b is a constant. As a simple consequence of this expression, we find that for $P_1/P_0 = \frac{1}{2}$ the other period ratios are equal to $P_k/P_0 = 1/(1 + k)$. It is this accumulation of the integer resonances which is the likely cause of the sharp, possibly discontinuous variation of the Fourier parameters for the low $T_{\rm eff}$ models of Figure 7.

8. Finally, we compare our results with those of previous nonlinear pulsational studies. The only work for which such a comparison can be carried out in a quantitative way is that of Hodson et al. (1982). Their models have been computed with the Los Alamos opacity tables, and they all have the same mass of 0.55 $M_\odot$. Two subsets of models; {B, C, D, E, J, L, N} and {F, G, H, I, O, P} scan sufficiently small ranges of luminosities (95–108 $L_\odot$ and 120–138 $L_\odot$, respectively) to be considered *approximate sequences* in our sense. Both these "sequences" are characterized by high values of ξ and consequently, in the resonance region their Fourier phases ϕ_{21} are rather low. For the second "sequence" which has approximately the same stellar parameters as our sequence D, the values of ϕ_{21} almost exactly coincide with ours. The amplitude ratio R_{21} for the first of the models is close to ours, but the remaining points fall somewhat low. The first "sequence" is akin to our sequence B. The Fourier phases ϕ_{21} for these models are slightly lower than in our calculations. The values of R_{21}, on the other hand, change with the pulsation period with a different slope, so that the first three points are below and the last two points are above the progression defined by our results. In general, however, the discrepancies between the model of this paper and the models of Hodson et al. (1982) are not very large, and they could be caused by small differences in the hydrocodes; however, they could also originate in the difference between the velocities of the outer zone, which we Fourier analyzed, and the interpolated, "photospheric" velocities, which Hodson et al. used.

3.3. *Amplitude Equations*

The radial velocity and light curves of the classical Cepheid models can be described fairly accurately by the amplitude equation formalism (KB89). In spite of the complicated variations of the Fourier parameters in the 2:1 resonance region, it is sufficient to include in the description only the first-order correction terms of the theory. The reason is to be found in the weakness of both the nonlinearity and of the dissipation in these models. In order to reinforce our statement that the 2:1 resonance also plays a dominant role in the BL Her variables, we also attempt to reproduce their behavior with the amplitude equations. An a priori success is not guaranteed, though, since the assumption of weak dissipation underlies the formalism, and the models are much more dissipative now than for the classical Cepheids. As in KB89, to which we refer the interested reader for the details and notation, the procedure consists of a fit rather than an ab initio calculation: First, it is assumed that all the *nonlinear* coefficients in the amplitude equations (Π_i, Re Q_i, Re T_i) are constant along the sequence when scaled with the period P_2. The linear coefficients, i.e.,

frequencies and growth rates are taken from the LNA analysis, and are thus known. Also assumed to be constant (with no scaling) are the coefficients h_{ij} appearing in the construction of the solution. Values of the nonlinear parameters are first guessed, then the amplitude equations are solved and the low-order Fourier coefficients are constructed. The nonlinear parameters are finally determined by a least-squares fit of the calculated Fourier coefficients to those obtained from the hydrodynamic data. The procedure is performed in two stages, first fitting A_1, ϕ_{21}, and R_{21}, and then ϕ_{31} and R_{31}.

In Figure 11 the resultant fit is shown for sequence A in which the 2:1 resonance is strong. The coefficients of this solution are given in Table 3, in the notation of KB89. The fit is seen to be good, especially for the Fourier phases ϕ_{21} and ϕ_{31}, although generally it is not as good as for the Cepheid sequences where the parameters A_1 and R_{21} were reproduced much better. The reason for the discrepancies could be the presence of additional resonances not included in the equations; we shall return to this point in the next section. We also remark that the BL Her sequence displayed in Figure 11 is considerably longer than any of the Cepheid sequences of KB89, and thus the assumption that the fitted parameters are constant along the sequence is "less justified." Despite these obvious shortcomings the 2:1 resonant amplitude equations *do capture* the main features of the Fourier parameter progression quite well. Interestingly, the fitted coefficients are not too different from those obtained for the Cepheid sequence B (shown in col. [3] of Table 3). Especially the low order, and thence best determined coefficients Π_0, Π_2, and h_{22} are very similar in both cases, and the important self-saturation coefficient Q_0 is within a factor of 2. Also the cubic expansion coefficients h_{23} and h_{33} are very close for both kinds of models. The only sizable difference is seen in the parameter Q_2 which, however, is always rather poorly determined from the fit. These results stress again a great similarity of our sequence A to the sequences of classical Cepheid models, a property already seen in Figures 3 and 5.

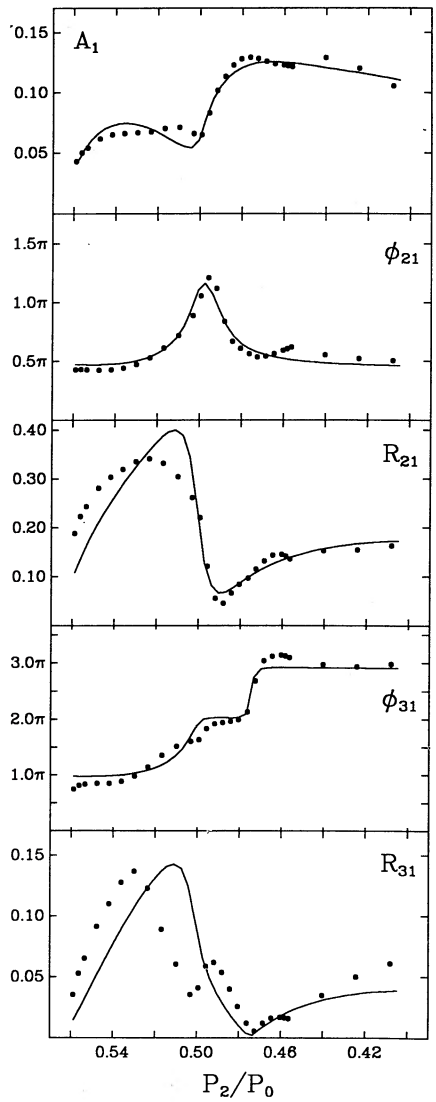

FIG. 11.—Amplitude equation fit for the Fourier parameters of the radius variations of the model sequence A. The fit is plotted as a solid line, the hydrodynamic data as dots.

The quality of the fit deteriorates rapidly for the BL Her sequences of higher luminosity; for sequence B it is still acceptable, but for C it is bad. This behavior is most likely a combination of the weakening of the resonance (increase of $|\kappa_2/\kappa_0|$) and the simultaneous increase of the dissipation of the models. The latter effect makes the amplitude equation formalism (which assumes *small* dissipation) less accurate in general, it also increases the size of the higher order terms which are neglected in the fit.

3.4. *3:1 Resonance*

Figures 5 and 6 indicate that sequences {A, B, D, E, F} show an additional, secondary minimum in the R_{31} progression which occurs slightly to the left of the primary minimum caused by the 2:1 resonance. The location of this additional dip correlates with the position of the 3:1 resonance between the fundamental mode and the fourth overtone, and it is therefore tempting to speculate that the feature is dynamically related to this resonance. In this subsection we shall argue that there is good evidence to support such an interpretation.

First, we compare the amplitude equation fit for the BL Her sequence A (Fig. 11) with that for the Cepheid sequence B (Figs. 1 and 3 of KB89). In the BL Her case, the major discrepancy between the analytical solution and the models occurs for

TABLE 3

PARAMETERS OF THE AMPLITUDE EQUATIONS FIT

Parameter (1)	BL Her (2)	Cepheids (3)
$\lvert\Pi_0\rvert P_2$	1.49	1.03
arg (Π_0)	4.57	4.56
$\lvert\Pi_2\rvert P_2$	0.37	0.54
arg (Π_2)	4.96	5.17
Re $Q_0 P_2$	−2.88	−1.41
Re $T_0 P_2$	−13.11	−18.40
Re $Q_2 P_2$	−11.81	−72.00
Re $T_2 P_2$	−12.50	−18.20
$\lvert h_{21}\rvert$	28.60	12.20
arg (h_{21})	5.53	5.96
$\lvert h_{22}\rvert$	2.10	2.77
arg (h_{22})	2.97	2.91
$\lvert h_{23}\rvert$	6.10	4.80
arg (h_{23})	3.14	3.14
$\lvert h_{33}\rvert$	5.62	7.00
arg (h_{33})	6.02	5.63

R_{21} and R_{31} and it is largest around $P_{20} = 0.51$. This is very close to the center of the 3:1 resonance, $\omega_4 = 3\omega_0$ which is located at $P_{20} = 0.513$. For the Cepheid sequence, the same 3:1 resonance lies at $P_{20} = 0.520$. Exactly at this place, the amplitude ratio R_{31} has again a pronounced minimum, and the ratio R_{21}, although much better captured by the amplitude equations, displays a small but noticeable wiggle. These features are not reproduced by the fit in which this 3:1 resonance is ignored. Secondary minima in the R_{31} progressions occur also in other Cepheid sequences (Fig. 9 of BMK). Their depth correlates with the relative damping of the resonant fourth overtone, $|\kappa_4/\kappa_0|$, viz. the more damped it is, the smaller the excursion in R_{31}. (In the BL Her models a similar correlation is difficult to see because the 2:1 and 3:1 resonances are much closer to each other.) Both for the BL Her and for the Cepheid sequences the discrepancies between the fit and the hydro results have the same signature: an unfitted minimum in R_{31} accompanied by a lowering of R_{21} with respect to the analytical model. Since in both cases these discrepancies are located in the vicinity of the 3:1 resonance, it is plausible that this additional coupling is responsible for the unfitted structures.

Further support for such an interpretation comes from Figure 8 which compares the BL Her sequence A with the Cepheid sequence D. As we have already mentioned, the Fourier progressions of both families of models are very similar for all the parameters *except* R_{31}. For this particular amplitude ratio the difference between the sequences can naturally be explained by the difference in the location of the 3:1 resonance. Because in Figure 4 we stretch the abscissa for the Cepheid models this resonance now appears at $P_{20} = 0.531$, instead of $P_{20} = 0.52$ (for the BL Her models it is at $P_{20} = 0.513$). We note that according to the amplitude equation formalism (Moskalik & Buchler 1989), a 3:1 coupling contributes to the ratio R_{31} already in the lowest order of the theory. Therefore, R_{31} *should be most affected* by the presence of such coupling, and the other (lower order) Fourier parameters should be only changed to a lesser extent. This is what is actually seen, pointing again at a 3:1 resonance as the reason for the variance between the sequences of Figure 8. The natural assumption that the resonance influences the BL Her and the Cepheid models in the same way also seems to explain qualitatively the small differences in the progressions of R_{21} which appears around $P_{20} = 0.51$ and $P_{20} = 0.535$. In both places, the lower values of R_{21} are displayed by the sequence in which the 3:1 resonance occurs. Analogous reasoning can be applied to the Fourier phases ϕ_{31} as well.

In principle, it should be possible to *fully* reproduce the variations of the Fourier parameters with the amplitude equations taking into account *both* the 2:1 resonance *and* the 3:1 resonance. We have attempted such a task for the Cepheid as well as for the BL Her models. The inclusion of the additional mode (the fourth overtone), though, increases the size of the nonlinear system to five equations, and totally, more than 20 coefficients have to be simultaneously determined. Unfortunately, such number of parameters turns out to be too large, and a meaningful fit can no longer be performed. The interesting 3:1 coupling terms which are cubic in the amplitudes (Moskalik & Buchler 1989) and, thus, of higher order than the 2:1 terms, are particularly difficult to converge.

3.5. *Period Doubling*

In Figures 4–7 we mark with open circles the models in which the usual limit cycle is unstable toward a period doubling perturbation. Such instability has been found in all studied BL Her sequences, except G. (The absence of open circles in sequence I is due to our inability to converge any of the unstable models to periodicity.) The instability is always limited to a rather narrow range of $T_{\rm eff}$ (typically 100–150 K) and, consequently, also to a narrow range of pulsation periods P_0 as shown in Table 4. In sequences A–F the bifurcation leads to stable period-two oscillations, in which all variables display RV Tau–like, albeit *strictly periodic*, alternations. This resembles the behavior encountered in the classical Cepheid models, where analogous windows of period-two pulsations have also been found (BMK; Moskalik & Buchler 1991; Moskalik, Buchler, & Marom 1992). Although we cannot be absolutely sure because of the coarseness of our effective temperature grid, it appears that in the sequences A–F only one period doubling occurs, and it is followed by a return to period-one cycles at lower $T_{\rm eff}$. On the other hand, in the two most dissipative (high ξ) sequences, H and I, a *series* of period doublings takes place, ending up in apparently irregular oscillations. This variability is very similar to the low dimensional chaotic behavior found in W Vir models by Buchler & Kovács (1987) and Kovács & Buchler (1988b). Contrary to the W Vir case, where the chaotic domain seems to be unbounded from the low-temperature side, in the BL Her sequences we find only narrow *windows* of irregular pulsations. These chaotic windows, though, may remain of academic interest only. Indeed, the sequence H has $L = 200\ L_\odot$, and the observational work of Demers & Harris (1974) suggests that Population II pulsators avoid this range of luminosities. The sequence I, on the other hand, is constructed with a mass of $M = 0.4\ M_\odot$ which is too low to represent realistically BL Her stars. In contrast, the regular period-two behavior occurs in models with proper masses, and with luminosities and periods placing them in a well populated part of the instability strip. Therefore, this behavior is interesting from an astrophysical point of view.

TABLE 4

PERIOD-TWO BL HER MODELS

Sequence	$T_{\rm eff}$ (K)	P_0 (days)
A	5600–5450	2.01–2.23
B	5850–5700	2.07–2.29
C	6000–5900	2.20–2.35
D	6000–5800	2.00–2.29
E	5700–5600	2.15–2.31
F	5600–5500	2.42–2.58
G	...[a]	...[a]
H	6350–6250	2.27–2.41
I	6360–6250	1.68–1.79

[a] Ellipse dots mean that there are no period-two solutions for these sequences.

In Figure 12 we present the radial velocity curves for the stable period-two limit cycles of sequences {A, B, C}. The curves are labeled with the $T_{\rm eff}$ of the static models (in [K]) and with the nonlinear pulsation period (in [days]) which are approximately twice the linear periods P_0. As in the case of period-two pulsations of Cepheid models (Moskalik & Buchler 1991), the alternations are most visible in the velocity minima. However, in contrast to the Cepheid case, these alternations are now *very pronounced* and can reach up to 30 km s^{-1} (or 21 km s^{-1} after the limb darkening correction). Thus they should be rather easily observable. According to our computations the phenomenon occurs in *all* BL Her sequences with $100\ L_\odot < L < 150\ L_\odot$ and $0.55\ M_\odot < M < 0.65\ M_\odot$, although the

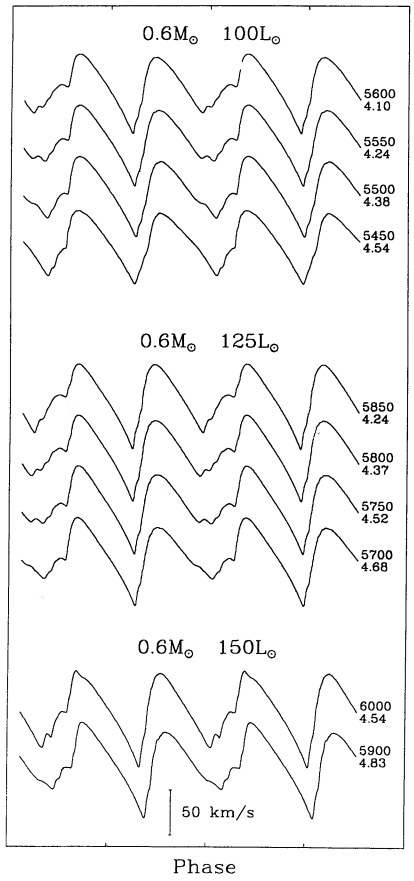

FIG. 12.—Radial velocity curves of period-two limit cycles of sequences A, B, and C. Labels denote $T_{\rm eff}$ [K] of the static models and the nonlinear pulsation periods [day].

range of P_0 where it happens *differs* from one sequence to another (cf. Table 4). We have also checked that the existence of the period-two pulsations is *very robust* with respect to the numerical parameters such as zoning, the integration time step or the pseudoviscosity. Therefore, we expect this behavior to be eventually found in the BL Her–type stars (Buchler & Moskalik 1990b).

The origin of the period doubling windows have already been discussed elsewhere (Moskalik & Buchler 1990; Buchler & Moskalik 1990a). Analytical work based on the amplitude equation formalism has unambiguously established that this behavior is caused by a *parametric instability* of an overtone in a *half-integer resonance*. In order to obtain a clue as to the resonance (and the mode) responsible for the period doubling in the BL Her case, we have resorted to a stability analysis of the limit cycles.

Figure 13 displays the Floquet coefficients of the lowest two overtones, computed for the models of sequence A. For convenience, we have introduced here the Floquet phases Φ_k and exponents λ_k, defined as $F_k \stackrel{\rm def}{=} \exp(\lambda_k + i\Phi_k)$, and have plotted them separately versus $T_{\rm eff}$. A secure association of the Floquet coefficients F_k with the linear eigenmodes is really possible only for models in the immediate vicinity of the blue edge (Hopf bifurcation). For such models Φ_k and λ_k coincide rather closely with the *linear* phases and exponents, given as $2\pi\omega_k/\omega_0$ and $2\pi\kappa_k/\omega_0$, respectively. Once the identification has been made at that point, it can then be continued toward lower $T_{\rm eff}$ for the rest of the sequence, provided that the grid in $T_{\rm eff}$ is sufficiently fine (typically 50–100 K or better; cf. Moskalik & Buchler 1990). We stress that this is the only proper procedure, and that the use of e.g., Floquet eigenvectors to discriminate between different modes is not reliable, particularly in the presence of resonances (Buchler, Moskalik, & Kovács 1991).

The identification of the Floquet coefficients is usually relatively easy for the first and the second overtones, but it becomes increasingly difficult and uncertain for the higher modes. In the BL Her models this problem is exacerbated because the coefficients for the third, fourth, and fifth overtones are almost indistinguishable. Therefore, we have decided to plot in Figure 13 the Φ_k and λ_k only for the two lowest order Floquet modes. For comparison, we also display by thin lines the linear phases (i.e., $\omega_k P_0$) of the corresponding modes. It is obvious from the definition that they go through zero at the integer resonances and through π at the half-integer ones. As we see, the Floquet phases closely track the linear phases, which is a testimony to the weakly nonlinear dynamical behavior of the limit cycles. (In contrast, the Floquet exponents are very different from the linear ones [not shown] because nonlinearity plays a large role in the dissipation.)

Figure 13 shows that for $T_{\rm eff}$ between $\sim$5800 and $\sim$5400 K a giant "bubble" forms in the Floquet exponent λ_1, accompanied by a plateau in the concomitant Floquet phase at $\Phi_1 = \pi$. Between $\sim$5600 K and $\sim$5450 K the bubble pierces the stability boundary $\lambda = 0$. This leads to the destabilization of the fundamental limit cycle and to the emergence of period-two oscillations. There is little doubt that the bubble (and thus the instability) is due to the 3:2 *resonance* between the fundamen-

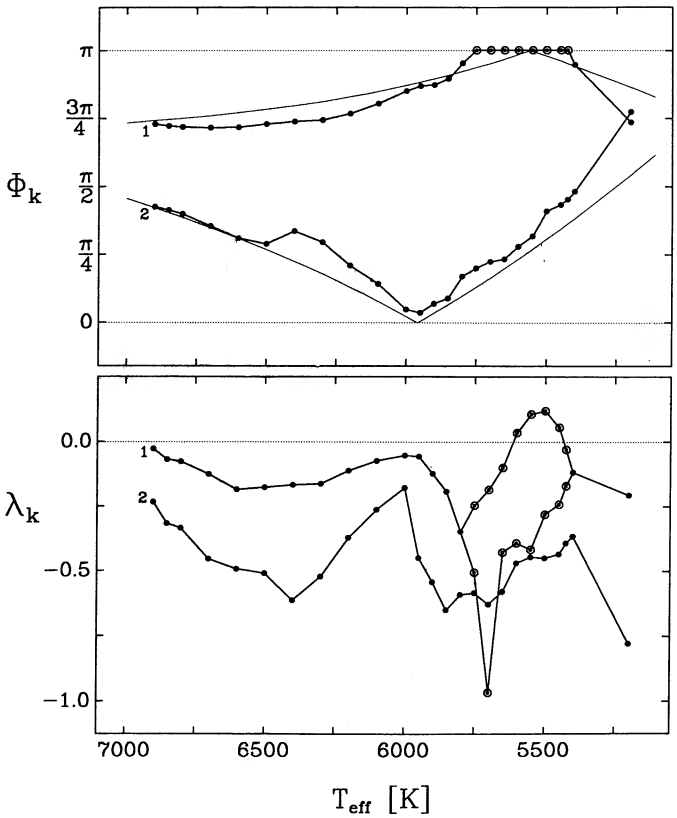

FIG. 13.—Floquet stability coefficients of the first and second overtone perturbations for models of sequence A. *Top:* Floquet phases; *bottom:* Floquet exponents. Thin lines denote linear phases (see text).

tal mode and the first overtone which occurs very near its center (cf. Table 2). The mechanism leading to such behavior is well captured by the amplitude equations and has been explained in detail elsewhere (Moskalik & Buchler 1990).

In other sequences, the period doubling windows still coincide with the 3:2 resonance, as shown by Tables 2 and 4. They become, though, somewhat shifted with respect to the resonance center, because of an increase in the nonadiabaticity and nonlinearity of the pulsations. Also, in sequences H and I where chaotic windows have been found, the same 3:2 coupling is responsible for the instability. This is in contrast to the W Vir models of Kovács & Buchler (1988b), in which chaotic behavior is caused by the 5:2 resonance between the fundamental and the second overtone (Moskalik & Buchler 1990).

At the end of this section, we want to report briefly some newly discovered, unexpected *hysteresis* behavior. In sequences D and E we have found the coexistence of stable period-one and period-two limit cycles. This behavior has been found over a remarkably narrow range of $T_{\rm eff}$, less than 10 K, to be precise. It is therefore quite possible that it may also happen in other sequences and that we have missed it. We note, for example, that in sequence A the size of the alternations in the radial velocity minima *does not decrease to zero* as the high-temperature edge of the period doubling window is approached (Fig. 4). This suggests that the bifurcation is subcritical and that hysteresis occurs. A further study of this phenomenon is in progress.

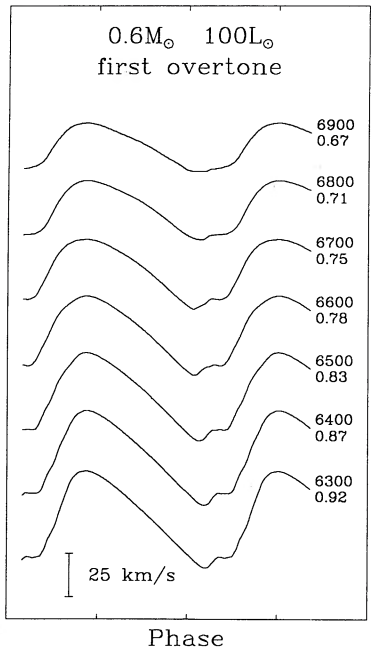

FIG. 14.—Radial velocity curves of the first overtone limit cycles of sequence A. Labels denote $T_{\rm eff}$ [K] of the static models and the nonlinear pulsation periods [day].

3.6. *Overtone Pulsations*

Up to this point we have only considered pulsations in the fundamental mode. However, over most of the studied range of $T_{\rm eff}$ the first overtone is also unstable and can give rise to a limit cycle. We have therefore computed periodic, nonlinear, first overtone pulsations for a few models of sequence A. The radial velocity curves of these limit cycles are shown in Figure 14. The curves are almost sinusoidal except for a small feature at the minimum. The lowest order Fourier parameters are approximately constant with $R_{21} \simeq 0.1$, $R_{31} \simeq 0.02$, $\phi_{21} \simeq \frac{1}{2}\pi$, and $\phi_{31} \simeq \frac{3}{4}\pi$. Nevertheless, a shallow minimum in both amplitude ratios can be noticed around $T_{\rm eff} \simeq 6600$ K which can possibly be related to the $\omega_4 = 2\omega_1$ resonance occurring near this place. The periods of the first overtone limit cycles are somewhat small for the BL Her stars and their velocity amplitudes are below what observations indicate. This seems to confirm the common belief that the BL Her variables are fundamental mode pulsators.

3.7. *Sensitivity to Artificial Viscosity*

In order to assess the sensitivity of the nonlinear pulsations to the artificial viscosity, we have recomputed sequence B with $C_Q = 6$ and $\alpha = 0.01$. A comparison of the low-order Fourier coefficients of the new models with the previous results shows that they agree generally to better than 5%. Only for one value does the small quantity R_{31} differ by 10%. This seems to be at odds with Simon (1988) who has found a strong sensitivity of his Fourier coefficients to the assumed value of the viscosity. We also mention that with $C_Q = 6$, the period doubling window still exists in sequence B in the same temperature range as before, but that the Floquet exponents are slightly lower.

4. DISCUSSION AND CONCLUSIONS

We have performed a fairly extended survey of sequences of hydrodynamical BL Herculis models. Our calculations show that the Fourier parameters of the radial velocity curves display the same kind of systematical progression with period or effective temperature, as seen in the models of classical Cepheids (cf. Buchler, Moskalik, & Kovács 1990). In particular, the Fourier phase ϕ_{21} has a well-defined maximum which is accompanied by a sharp decline of the concomitant amplitude ratio R_{21}. The progression is indubitably associated with the 2:1 resonance between the fundamental mode and the second overtone, just as for the classical Cepheids. Not only is the ϕ_{21} peak located near the resonance center and its height strongly correlated with the damping of the overtone, but, in addition, the Fourier parameter curves for different sequences become similar, when plotted versus P_2/P_0 (but not vs. P_0!). Also the variations of the Fourier coefficients can be fitted with the amplitude equations, but again, *only* when the 2:1 resonance is included.

For the low-luminosity sequences the effects of the 2:1 resonance are very pronounced, and the similarity of Fourier progressions between the BL Her and the Cepheid models is very close, even in a *quantitative* sense. With an increase in the luminosity, though, the role of the resonance gradually diminishes and the range of variation of ϕ_{21}, as well as of the other Fourier parameters, becomes smaller. The same trend is also seen when the masses of the models are lowered. These changes in the morphology of the phase and amplitude ratio curves are *significantly larger* than in the Cepheid case. As a result, for models exploring the whole observationally acceptable range of M and L, no "universal" ϕ_{21} versus P_2/P_0 relation can be established.

For the classical Cepheids the Fourier parameters of the observed radial velocity curves display very regular behavior as a function of the pulsation period (Kovács, Kisvarsányi, & Buchler 1990). There are several reasons why we should not expect to see such a simple behavior in the BL Her stars. First, as just mentioned, the strength of the 2:1 coupling depends very sensitively on the stellar mass and luminosity. Both

parameters can vary independently because there is no constraining evolutionary M-L relation. Second, changing M and L we also significantly change the position of the resonance. For the luminosities between 100 $L_\odot$ and 150 $L_\odot$, for example, it can be located anywhere between $1^d.58$ and $1^d.82$. Because of these two effects, at any given period, we can find stars with *different* shapes of the radial velocity curves. Third, resonances other than $\omega_2 = 2\omega_0$ also affect the BL Her pulsations. The 3:1 coupling with the fourth overtone, for example, creates a secondary minimum in the progression of R_{31} (this resonance has already been mentioned by Petersen 1989.) Compared to the Cepheids, the BL Her variables have period ratios that are much steeper functions of the period, so that the resonances are more crowded. Additionally, the width of the instability strip is thought to be $\sim$1400 K or more (Demers & Harris 1974), whereas for Cepheids it is significantly smaller (cf. e.g., discussion of Buchler, Moskalik, & Kovács 1990). Thus we can expect that for the BL Her stars many resonances are located inside the instability strip and, consequently, more complicated variations of the Fourier coefficients with period are possible.

In all studied sequences except one, we have encountered narrow ranges of $T_{\rm eff}$ in which the instability toward a period doubling bifurcation occurs. This instability is caused by the 3:2 resonance between the fundamental mode and the first overtone. In the two most nonadiabatic sequences chaotic behavior emerges, but in other cases only a single period doubling takes place. The nascent period-two oscillations are characterized by pronounced, strictly periodic alternations of the light and the radial velocity curves. The phenomenon appears for periods between $2^d.0$ and $2^d.6$. The exact range varies with the stellar parameters, though, and in no sequence is it broader than $0^d.3$. For $L \geq 125\ L_\odot$, models with such periods are located well within the observational instability strip. The alternations are always very robust with respect to numerical as well as physical parameters. They are also found to be quite large, exceeding 20 km s^{-1} in the velocity minima. Thus the behavior should be easily observable.

The model calculations discussed in the present paper unfortunately cannot be compared with observations at this time, since practically no data of good quality are available for the BL Her velocity curves. There exists enough theoretical material now to make a systematical observational program a worthwhile effort. The accurate measurement of velocity curves for a large sample of BL Her variables would be especially desirable because the Fourier parameters for these stars are sensitive to mass and to luminosity. Such measurements therefore could allow a determination of M and L for many of these objects.

The observational situation for the brightness variations of the BL Her stars is better, and several high-quality light curves have been published. There are also about three dozen stars for which the Fourier parameters have been determined (Petersen & Diethelm 1986). In a following paper we shall discuss the light curves of our BL Her models and compare them with the available data.

It is a great pleasure to acknowledge fruitful discussions with Géza Kovács. This work has been supported by NSF (grants AST 86-10027 and AST 89-14425), by the Pittsburgh Supercomputing Center, and by an RCI grant through IBM and the NE Regional Data Center at the University of Florida.

REFERENCES

Abt, H. A., & Hardie, R. H. 1960, ApJ, 131, 155
Barnes, T. G., Moffett, T. J., & Slovak, M. H. 1988, ApJS, 66, 43
Becker, S. A. 1985, in IAU Colloq. 82, Cepheids: Theory and Observations, ed. B. F. Madore (Cambridge: Cambridge Univ. Press), 104
Buchler, J. R. 1985, in NATO ASI Series C161, Chaos in Astrophysics, ed. J. R. Buchler, J. Perdang, & E. A. Spiegel (Dordrecht: Reidel), 137
———. in NATO ASI Ser. C302, The Numerical Modelling of Nonlinear Stellar Pulsations: Problems and Prospects, ed. J. R. Buchler (Dordrecht: Kluwer), 1
Buchler, J. R., & Goupil, M.-J. 1984, ApJ, 279, 394
Buchler, J. R., & Kovács, G. 1986, ApJ, 303, 749
———. 1987, ApJ, 320, L57
Buchler, J. R., & Moskalik, P. 1990a, in NATO ASI Ser. C302, The Numerical Modelling of Nonlinear Stellar Pulsations: Problems and Prospects, ed. J. R. Buchler (Dordrecht: Kluwer), p. 143
———. 1990b, in ASP Conf. Ser., Vol. 11, Confrontation Between Stellar Evolution and Pulsation, ed. C. Cacciari & G. Clementini (San Francisco: ASP), 383
Buchler, J. R., Moskalik, P., & Kovács, G. 1990, ApJ, 351, 617 (BMK)
———. 1991, ApJ, 380, 185
Carson, T. R., & Lawrence, S. P. A. 1987, in Stellar Pulsations, ed. A. N. Cox, W. M. Sparks, & S. G. Starrfield (New York: Springer), 293
Carson, T. R., & Stothers, R. 1982, ApJ, 259, 740
Carson, T. R., Stothers, R., & Vemury, S. K. 1981, ApJ, 244, 230
Cox, A. N. 1984, in Theoretical Problems in Stellar Stability and Oscillations, ed. A. Noels & M. Gabriel (Liège: Univ. of Liège), 1
Cox, A. N., & Kidman, R. B. 1985, in IAU Colloq. 82, Cepheids: Theory and Observations, ed. B. F. Madore (Cambridge: Cambridge Univ. Press), 250
Demers, S., & Harris, W. E. 1974, AJ, 79, 627
Harris, H. C. 1985, in IAU Colloq. 82, Cepheids: Theory and Observations, ed. B. F. Madore (Cambridge: Cambridge Univ. Press), 232
Harris, H. C., & Wallerstein, G. 1984, AJ, 89, 379
Hertzsprung, E. 1926, Bull. Astron. Inst. Netherlands 3, 115
Hodson, S. W., Cox, A. N., & King, D. S. 1982, ApJ, 253, 260
King, D. S., Cox, A. N., & Hodson, S. W. 1981, ApJ, 244, 242
Klapp, J., Goupil, M.-J., & Buchler, J. R. 1985, ApJ, 296, 514
Kovács, G. 1990, in NATO ASI Ser. C302, The Numerical Modelling of Nonlinear Stellar Pulsations; Problems and Prospects, ed. J. R. Buchler (Dordrecht: Kluwer), 73
Kovács, G., & Buchler J. R. 1988a, ApJ, 324, 1026
———. 1988b, ApJ, 334, 971
———. 1989, ApJ, 346, 898 (KB89)
Kovács, G., Kisvarsányi, E., & Buchler, J. R. 1990, ApJ, 351, 606
Ledoux, P., & Walraven, T. 1958, in Handbuch der Physik, Vol. 51, ed. S. Flugge (Berlin: Springer) 353
Moskalik, P., & Buchler, J. R. 1989, ApJ, 341, 997
———. 1990, ApJ, 355, 590
———. 1991, ApJ, 366, 300
Moskalik, P., Buchler, J. R., & Marom, A. 1992, ApJ, 385, 685
Petersen, J. O. 1981, A&A, 96, 146
———. 1989, A&A, 226, 151
Petersen, J. O., & Diethelm, R. 1986, A&A, 156, 337
Simon, N. R. 1986, ApJ, 311, 305
———. 1988, in Pulsation and Mass Loss in Stars, ed. R. Stalio & L. A. Willson (Dordrecht: Kluwer), 27
Simon, N. R., & Lee, A. S. 1981, ApJ, 248, 291
Simon, N. R., & Moffett, T. J. 1985, PASP, 97, 1078
Simon, N. R., & Sastri, V. K. 1972, A&A, 21, 39
Simon, N. R., & Schmidt, E. G. 1976, ApJ, 205, 162
Stellingwerf, R. A. 1974, ApJ, 192, 139
———. 1975, ApJ, 195, 441
Stobie, R. S. 1973, Observatory, 93, 111
Stobie, R. S., & Balona, 1979, MNRAS, 189, 641
Wallerstein, G. 1990, in ASP Conf. Ser., Vol. 11, Confrontation between Stellar Evolution and Pulsation, ed. C. Cacciari & G. Clementini (San Francisco: ASP), 56
Wallerstein, G., & Brugel, E. W. 1979, AJ, 84, 1840
Wallerstein, G., & Cox, A. N. 1984, PASP, 96, 677